Crystallization Behavior of Carbon Black-Filled Polypropylene and Polypropylene/Epoxy Composites

Ying Li, Shifeng Wang, Yong Zhang, Yinxi Zhang

Research Institute of Polymer Materials, Shanghai Jiao Tong University, Shanghai 200240, People's Republic of China

Received 27 April 2005; accepted 19 September 2005
DOI 10.1002/app.23254
Published online in Wiley InterScience (www.interscience.wiley.com).

ABSTRACT: The crystallization behavior of polypropylene (PP)/carbon black (CB) and PP/epoxy/CB composites was studied with differential scanning calorimetry (DSC). The effects of compatibilizer MAH-*g*-PP and dynamic cure on the crystallization behavior are investigated. The nonisothermal crystallization parameters analysis showed that CB particles in the PP/CB composites and the dispersed epoxy particles in the PP/epoxy composites could act as nucleating agents, accelerating the crystallization of the composites. Morphological studies indicated that the incorporation of CB into PP/epoxy resulted in its preferential localization in the epoxy resin phase, changing the spherical epoxy particles into elongated structure, and thus reduced the nucleation effect of epoxy particles. Addition of MAH-*g*-PP significantly decreased the average diameter of epoxy particles in the PP/epoxy and PP/epoxy/CB composites, promoting the crystallization of PP more effectively. The isothermal crystallization kinetics and thermodynamics of the PP/CB and PP/epoxy/CB composites were studied with the Avrami equation and Hoffman theory, respectively. The Avrami exponent and the crystallization rate of the PP/CB composites were higher than those of PP, and the free energy of chain folding for PP crystallization decreased with increasing CB content. Addition of MAH-*g*-PP into the PP/epoxy and PP/epoxy/CB composites increased the crystallization rate of the composites and decreased the chain folding energy significantly. © 2006 Wiley Periodicals, Inc. J Appl Polym Sci 102: 104–118, 2006

Key words: poly(propylene); epoxy resin; carbon black; crystallization; morphology

INTRODUCTION

Polypropylene (PP) is a versatile semicrystalline thermoplastic of high consumption because of its easy processability, relatively low cost, and especially its well-balanced physical and mechanical properties. Physical properties of polymer materials strongly depend on their microstructure and crystallinity, since it is at this microscopic level where the failure of the materials occurs.[1] Presently, the studies concerning the crystallization behavior of PP have been carried out extensively.

The crystallization behavior of PP can be obviously modified by the presence of another polymer component or fillers. Arroyo et al.[2] reported that the particles of ethylene–propylene–diene rubber (EPDM) in PP/EPDM blends acted as nucleating agents at low EPDM content (<25%), accelerating the crystallization of PP. But at higher EPDM content, the EPDM obstructed the mobility of PP chains and decreased the PP crystallization rate. Similar results were obtained by Lopez-Manchado et al.[3,4] Previous studies in our laboratory showed that the dispersed polycarbonate[5] or dynamically cured epoxy resin[6] particles in the PP matrix could act as nucleating agents and accelerated the crystallization rate of the PP component in the composites. Saroop and Mathur[7] found that the butadiene–styrene block copolymer could act as a nucleating agent for PP crystallization. Various inorganic or polymeric fibers such as glass fibers,[3,8,9] carbon and polytetrafluorethylene fibers,[10] polyethylene terephthalate fibers,[3,10,11] and aramid fibers[2,11] have been reported to be effective nucleating agents for PP crystallization, giving rise to the phenomenon of PP transcrystallinity on their surface. Inorganic fillers often act as nucleating agents for PP crystallization, such as talc,[12,13] nano-SiO_2,[14] $Mg(OH)_2$,[15] carbon nanotube,[16] and clay.[17] The crystallization kinetics of PP have hitherto been widely studied with different methods,[12–14,18] and in general, have been successfully described by the Avrami equation.[1,8]

Carbon black (CB) is one of the most widely used inorganic fillers in polymers. Because of its abundant source, low density, permanent conductivity, and low cost, CB has long been used as a conductive filler to decrease the electrical resistivity of insulating polymers or polymer blends and fabricate conductive polymer composites (CPCs).[19–22] To date, the most important aspects of the CPCs based on CB-filled PP or PP/another polymer blends that have been investigated are related to the electrical properties and mor-

Correspondence to: Y. X. Zhang (yxzhang@sjtu.edu.cn).

phology of the composites.[21,23–27] However, little research has been carried out on the crystallization behavior of CB-filled conductive PP composites in detail.[25,26]

We have prepared CB-filled CPCs based on PP and PP/epoxy blends by melt-mixing method. In the present study, the crystallization behavior of PP/CB and PP/epoxy/CB composites was examined with differential scanning calorimetry (DSC). The isothermal crystallization kinetics and thermodynamics of PP in the composites were studied with the Avrami equation and Hoffman theory, respectively. The effect of addition of CB, compatibilizer, and curing agent on the morphology and crystallization of PP in the PP/epoxy/CB composites was investigated.

EXPERIMENTAL

Materials

PP (M1600) was produced by Hyundai Petrochemical (Seoul, Korea), with a melt-flow index (MFI) of 25 g/10 min. Electrically conductive CB (V-XC72) was provided by Cabot (Pampa, TX), with DBP absorption of 168.6 mL/100 g and average diameter of 30 nm. Diglycidyl ether of bisphenol A resin (weight-average molecular weight = 4500 g/mol) was produced by Shanghai Resin (Shanghai, People's Republic of China). 2-Ethylene-4-methane-imidazole (EMI-2,4), supplied by Shanghai Chemical Agent (Shanghai, People's Republic of China), was used as the curing agent. MAH-*g*-PP with a maleic anhydride content of 1% was produced by Shanghai Sunny New Technology Development (Shanghai, People's Republic of China).

Sample preparation

Prior to blending, all materials were dried at 80°C in vacuum for about 8 h. Unless otherwise specified, the PP/CB and PP/epoxy/CB composites were prepared by melt mixing of the dry blended components in a Haake RC90 Rheometer (Karlsruhe, Germany) at 190°C and 30 rpm. For the samples containing compatibilizer MAH-*g*-PP, MAH-*g*-PP and PP were initially mixed for 2 min, and then the epoxy resin and CB were added. For the dynamically cured samples, the curing agent (EMI-2,4) was added after the addition of epoxy resin and CB as the mixing continued, as the procedure depicted in the literature.[6] The total mixing time was about 10 min. All blend ratios described are related to weight ratios. The resultant composites were subsequently compression molded at 190°C to prepare plaques for testing.

DSC analysis

The crystallization behavior of PP in the composites prepared was analyzed using a PerkinElmer Pyris 1 Differential Scanning Calorimeter (Boston, MA) under a nitrogen atmosphere. Samples of about 4 mg were taken from the molded plaques. Nonisothermal crystallization studies were performed as follows: the samples were heated to 200°C at a heating rate of 10°C/min, maintained at this temperature for 5 min to eliminate any previous thermal history, and then cooled to 50°C at a cooling rate of 10°C/min. Isothermal crystallization studies were performed as follows: the thermal history of the samples was removed as for the nonisothermal crystallization, and then the samples were cooled rapidly (100°C/min) to the crystallization temperature (T_c) and maintained at that temperature for the time necessary for the complete crystallization of the PP matrix. Five T_c values of 128, 131, 134, 137, and 140°C were chosen for the isothermal crystallization studies. The heat evolved during the isothermal crystallization was recorded as a function of time at different T_c's. After crystallization, the samples were heated to 200°C at a rate of 10°C/min and the melting temperatures (T_m) of the composites were recorded.

Scanning electron microscopy analysis

The samples were fractured in liquid nitrogen and the freeze-fractured surfaces were observed with a Hitachi S-2150 scanning electron microscope (Tokyo, Japan). All samples were gold sputtered prior to observation.

RESULTS AND DISCUSSION

Nonisothermal crystallization parameters

From the DSC crystallization exotherms recorded as the samples were crystallized from the molten state at a given cooling rate, some useful parameters can be obtained to describe the nonisothermal crystallization.[7,28] These parameters are defined below and illustrated in Figure 1.

T_p: The peak temperature of crystallization exotherm.

$T_{onset} - T_p$: The inverse measure of the overall rate of crystallization, where T_{onset} is the temperature at the intercept of the tangents at the baseline and the high-temperature side of the exotherm. The smaller the $T_{onset} - T_p$, the greater the rate of crystallization is.

S_i: Slope of initial portion of the exotherm, which is a measure of the rate of nucleation.[28] The greater the initial slope, the faster the nucleation rate is.

ΔW: The width at half-height of the exotherm peak determined after normalization of the peak to a constant mass of the samples, which is a measure of the crystallite size distribution. The narrower the crystallite size distribution, the smaller will be ΔW.

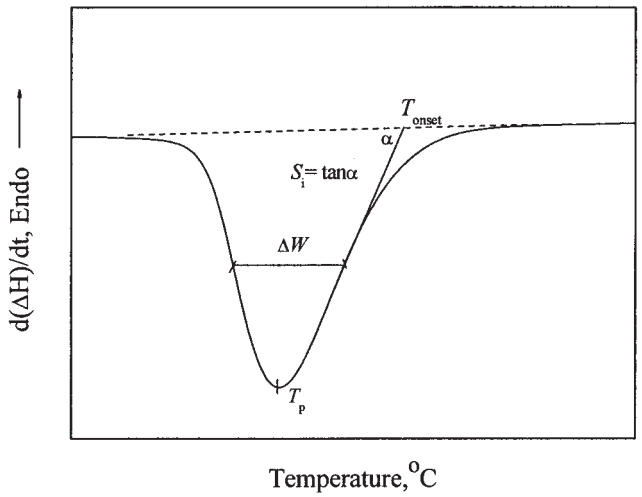

Figure 1 Schematic representation of the nonisothermal crystallization parameters determined from DSC crystallization exotherm.

Nonisothermal crystallization of PP and the PP/CB composites

DSC cooling thermograms of PP and PP/CB composites and their normalized DSC cooling thermograms in the region of crystallization are shown in Figures 2(a) and 2(b), respectively. A summary of the nonisothermal crystallization parameters determined from the normalized DSC thermograms is given in Table I. All the T_p values of the PP/CB composites are higher than that of pure PP (117.0°C), and T_p increases with increasing CB content. At low CB content (2.0 phr), T_p increases slightly. After CB content reaches 5.3 phr, T_p values of the PP/CB composites increase more obviously. At a CB content of 10.0 phr, T_p is increased by 4.5°C with respect to that of PP. However, there is little increase of T_p when the CB content is beyond 10.0 phr. All the $T_{onset} - T_p$ values of the PP/CB composites are smaller than that of pure PP, indicating that the addition of CB into PP increased the overall rate of crystallization of PP. The $T_{onset} - T_p$ values of the PP/CB composites decrease with increasing CB content. But, after CB content reaches 5.3 phr, the $T_{onset} - T_p$ values vary slightly.

The parameters of the rate of nucleation (S_i) and the crystallite size distribution (ΔW) are also listed in Table I. S_i of all PP/CB composites are greater than that of pure PP, implying that the PP/CB composites have higher rate of nucleation. At a low CB content of 2.0 phr, S_i increases slightly. After CB content reaches 5.3 phr, the S_i values increased greatly, and the S_i value of PP filled with 5.3 phr CB is the greatest. ΔW of 2.0-phr CB-filled PP slightly decreased with respect to that of PP. Increasing CB content results in the great decrease of ΔW, indicating that the crystallite size distribution of the PP/CB composites is more uniform than that of PP when CB content is higher than 5.3 phr.

Analysis of the data in Table I shows that CB particles can act as effective nucleating agents, increasing the peak temperature and the overall rate of the crystallization of PP. The addition of CB into PP increases the rate of nucleation and narrows the crystallite size distribution. At low CB content, the nucleating effect of CB is small. The nucleating effect of CB is prominent at CB content between 5.3 and 10.0 phr. Higher CB content has little enhancement effect on the crystallization of PP. This is consistent with the study of

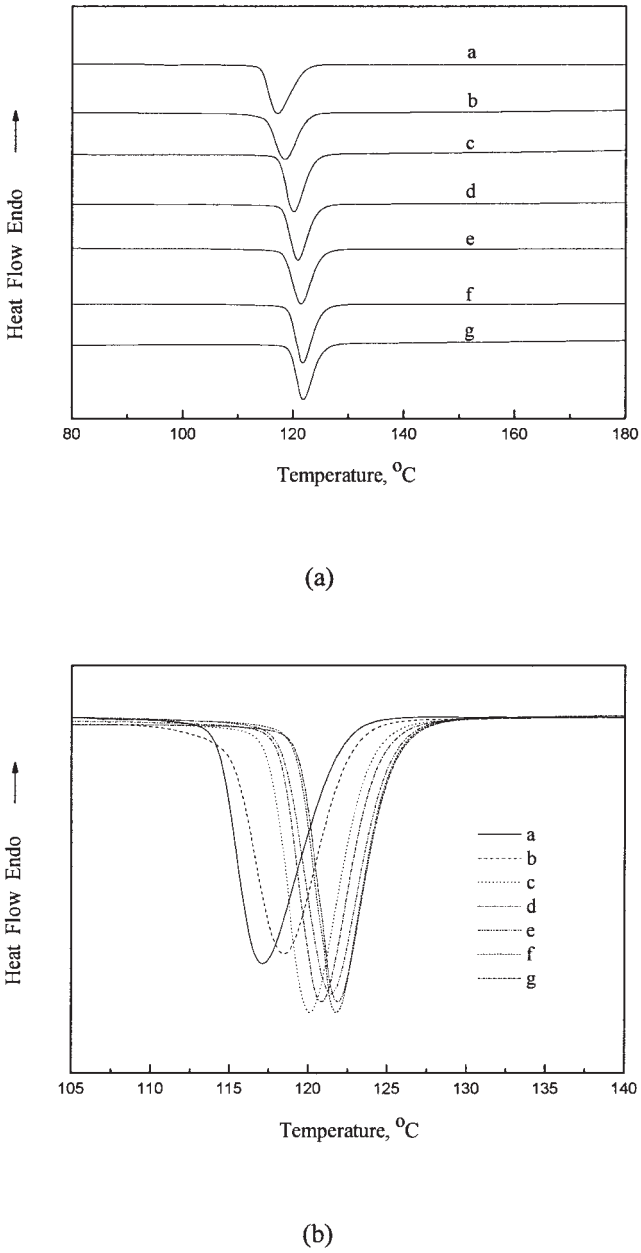

Figure 2 (a) DSC thermograms and (b) normalized DSC thermograms recorded during nonisothermal crystallization at a cooling rate of 10°C/min of a –PP and PP/CB composites with varied CB content, b –2.0 phr, c –5.3 phr, d –8.7 phr, e –10.0 phr, f –17.7 phr, and g –25.0 phr.

TABLE I
Various Parameters of PP and the PP/CB Composites Determined from the Nonisothermal Crystallization Exotherm at a Cooling Rate of 10 °C/min

Composition	T_p (°C)	T_{onset} (°C)	$T_{onset} - T_p$ (°C)	S_i	ΔW
PP	117.0	122.0	5.0	2.76	4.6
PP/CB (100/2.0)	118.5	122.6	4.1	2.83	4.5
PP/CB (100/5.3)	120.2	123.8	3.6	3.82	3.8
PP/CB (100/8.7)	120.8	124.3	3.5	3.54	3.4
PP/CB (100/10.0)	121.5	125.1	3.6	3.54	3.8
PP/CB (100/17.7)	121.7	125.2	3.5	3.76	3.4
PP/CB (100/25.0)	121.8	125.3	3.5	3.66	3.3

Mucha et al.[25] that concluded that the diffusion of crystallizing macromolecules was restricted in the crystallization front by increasing the concentration of rejected CB particles.

Nonisothermal crystallization of the PP/epoxy and PP/epoxy/CB composites

Figure 3(a) shows the DSC cooling thermograms of the PP/epoxy and PP/epoxy/CB composites, and the normalized DSC cooling thermograms in the region of crystallization are shown in Figure 3(b). The thermogram of PP is also depicted in Figure 3 for comparison. Data of the nonisothermal crystallization parameters determined from the normalized DSC thermograms are listed in Table II. T_p of PP/epoxy (70/30) is 4.2°C higher than that of pure PP. Addition of CB into PP/epoxy (70/30) results in decreased T_p values, which are slightly higher than that of PP. And T_p increases with increasing CB content in the CB-filled PP/epoxy (70/30) composites. For the dynamically cured PP/epoxy and PP/epoxy/CB composites, the T_p values are slightly lower than that of the corresponding uncured composites. Similarly, the addition of CB results in lower T_p of PP/epoxy/CB/EMI-2,4 (70/30/6.4/1.2) than that of PP/epoxy/EMI-2,4 (70/30/1.2). Addition of compatibilizer (MAH-*g*-PP) into PP/epoxy and PP/epoxy/CB increases the T_p values significantly, by more than 13°C with respect to that of PP. And T_p of PP/MAH-*g*-PP/epoxy/CB (60/10/30/6.4) is slightly higher than that of PP in PP/MAH-*g*-PP/epoxy (60/10/30). For their dynamically cured composites, the T_p values are significantly higher than that of pure PP, but slightly lower than that of the corresponding uncured composites. Similarly, the T_p value of PP/MAH-*g*-PP/epoxy/CB/EMI-2,4 (60/10/30/6.4/1.2) is slightly higher than that of PP/MAH-*g*-PP/epoxy/EMI-2,4 (60/10/30/1.2).

All the $T_{onset} - T_p$ values of the PP/epoxy and PP/epoxy/CB composites are smaller than that of pure PP, indicating that the overall rate of crystallization of the composites are faster than that of pure PP. For the PP/epoxy (70/30) filled with varied CB content, the $T_{onset} - T_p$ values decrease with increasing CB content. For the PP/epoxy and PP/epoxy/CB composites containing MAH-*g*-PP, the $T_{onset} - T_p$ values are small and vary slightly with composition. All

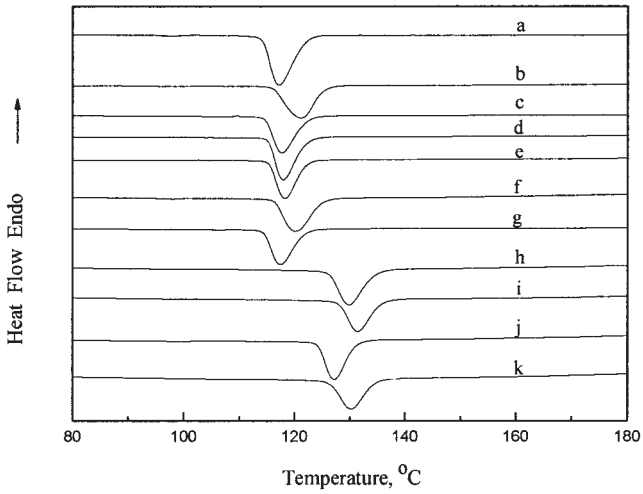

(a)

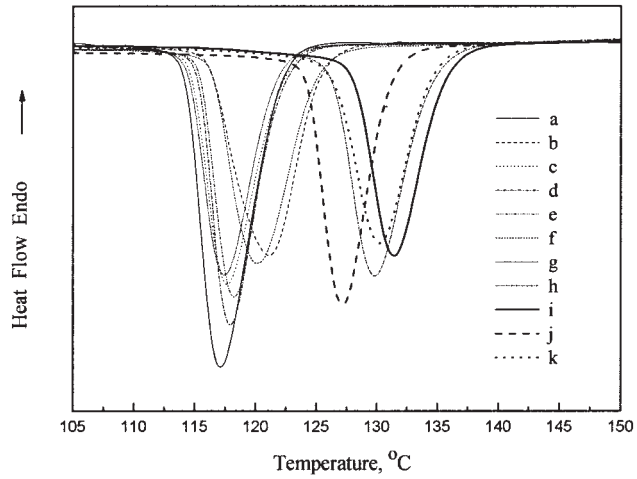

(b)

Figure 3 (a) DSC thermograms and (b) normalized DSC thermograms of PP, PP/epoxy, and PP/epoxy/CB composites recorded during nonisothermal crystallization at a cooling rate of 10°C/min: a –PP, b –PP/epoxy (70/30), c –PP/epoxy/CB (70/30/2.0), d –PP/epoxy/CB (70/30/4.0), e –PP/epoxy/CB (70/30/6.4), f –PP/epoxy/EMI-2,4 (70/30/1.2), g –PP/epoxy/CB/EMI-2,4 (70/30/6.4/1.2), h –PP/MAH-*g*-PP/epoxy (60/10/30), i –PP/MAH-*g*-PP/epoxy/CB (60/10/30/6.4), j –PP/MAH-*g*-PP/epoxy/EMI-2,4 (60/10/30/1.2), and k –PP/MAH-*g*-PP/epoxy/CB/EMI-2,4 (60/10/30/6.4/1.2).

TABLE II
Various Parameters of PP, PP/Epoxy, and PP/Epoxy/CB Composites Determined from the Nonisothermal Crystallization Exotherm at a Cooling Rate of 10 °C/min

Composition	T_p (°C)	T_{onset} (°C)	$T_{onset} - T_p$ (°C)	S_i	ΔW
PP	117.0	122.0	5.0	2.76	4.6
PP/epoxy (70/30)	121.2	125.3	4.1	1.89	6.3
PP/epoxy/CB (70/30/2.0)	117.7	122.2	4.5	1.94	4.5
PP/epoxy/CB (70/30/4.0)	117.9	122.0	4.1	2.56	4.0
PP/epoxy/CB (70/30/6.4)	118.2	122.0	3.8	2.43	3.9
PP/epoxy/EMI-2,4 (70/30/1.2)	120.3	125.0	4.7	1.80	5.0
PP/epoxy/CB/EMI-2,4 (70/30/6.4/1.2)	117.5	121.7	4.2	2.05	4.3
PP/MAH-*g*-PP/epoxy (60/10/30)	130.1	134.3	4.2	1.84	4.6
PP/MAH-*g*-PP/epoxy/CB (60/10/30/6.4)	131.4	135.6	4.2	1.85	4.5
PP/MAH-*g*-PP/epoxy/EMI-2,4 (60/10/30/1.2)	127.0	131.3	4.3	2.41	3.9
PP/MAH-*g*-PP/epoxy/CB/EMI-2,4 (60/10/30/6.4/1.2)	130.2	134.5	4.3	1.76	4.7

dynamically cured composites show greater $T_{onset} - T_p$ values than the corresponding uncured composites.

The S_i and ΔW values of the PP/epoxy and PP/epoxy/CB composites vary with the compositions. Generally, the smaller the S_i, the greater the ΔW is. A similar result was reported by Saroop and Mathur.[7] They explained that the slower rate of nucleation could cause formation of large spherulites while formation of some smaller spherulites could also take place. The coexistence of small and large crystallites for the PP phase of the composites resulted in a wider crystallite size distribution. PP/epoxy (70/30) and PP/epoxy/EMI-2,4 (70/30/1.2) show relatively small S_i and great ΔW values.

Morphology of the PP/epoxy and PP/epoxy/CB composites

The crystallization behavior of the polymer blends composed of PP and another polymer is related to the morphology of the polymer blends.[5,6] Figure 4 shows scanning electron microscopy (SEM) micrographs of the freeze-fractured surface of PP, PP/epoxy, and PP/epoxy/CB composites. In PP/epoxy (70/30), the epoxy resin forms dispersed spherical particles in the PP matrix (Fig. 4(b)). The average diameter of most epoxy particles is about 3–6 μm, but there are also some larger epoxy particles of more than 10 μm in diameter. The epoxy particles can act as nucleating agents, accelerating the crystallization of the PP component. This is supported by the increase in T_p and decrease in the $T_{onset} - T_p$ values, as shown in Table II.

Addition of CB into PP/epoxy results in the preferential localization of CB in the epoxy phase, changing the spherical particles of epoxy resin into elongated structures, as shown in Figures 4(c) and 4(d). Studies on CB-filled CPCs have shown the distribution of CB in polymer blends is mainly determined by the polarity of the polymer matrix.[22–24] CB has a tendency to locate preferentially in the phase exhibiting higher percolation threshold when blending with CB individually, usually the phase of higher polarity. The percolation threshold is referred to as the critical content of CB required to form continuous conducting paths and impart electrical conductivity to the polymer matrix. Miyasaka et al.[20] reported that the higher the polarity of a given polymer, the larger the critical content of CB was. Because the polymer of higher polarity can readily wet the CB particles, showing stronger affinity to CB, and thus higher CB contents are needed to achieve conductivity when mixed with the polymer individually.[23] In our present work, the preferential localization of CB in epoxy is consistent with the results of those studies. The percolation threshold of epoxy/CB is about 17 phr CB, much higher than that of the PP/CB composite, which is about 8 phr CB. PP is a nonpolar polymer, whereas epoxy resin is a polar resin. The higher polarity of epoxy resin makes it easily wet CB, i.e., CB has a stronger affinity to epoxy than to PP. Formation of elongated structure of the dispersed phase due to the addition of CB has been previously reported,[22,24] which was attributed to the reduced interfacial interaction or the interphase friction between the CB-coated dispersed particles and the matrix.

Addition of CB into PP/epoxy leads to the formation of elongated structure of most dispersed epoxy particles, and only a few spherical epoxy particles can be seen in Figure 4(c). As a result, the nucleation effect of epoxy particles is greatly reduced, and the T_p values of CB-filled PP/epoxy (70/30) are lower than that of the unfilled blend. For PP/epoxy (70/30) filled with varied CB content, it can be deduced from Table II that with increasing CB content, T_p increases slightly and the $T_{onset} - T_p$ value decreases. This phenomenon may be related to the CB distribution at varied CB content. At 2 or 4 phr CB, the CB content is lower than the percolation threshold in the epoxy phase (5.1 phr for 30% epoxy in the PP/epoxy blend). CB preferentially locates in epoxy, forming elongated structure. When CB saturated the polymer phase with stronger affinity

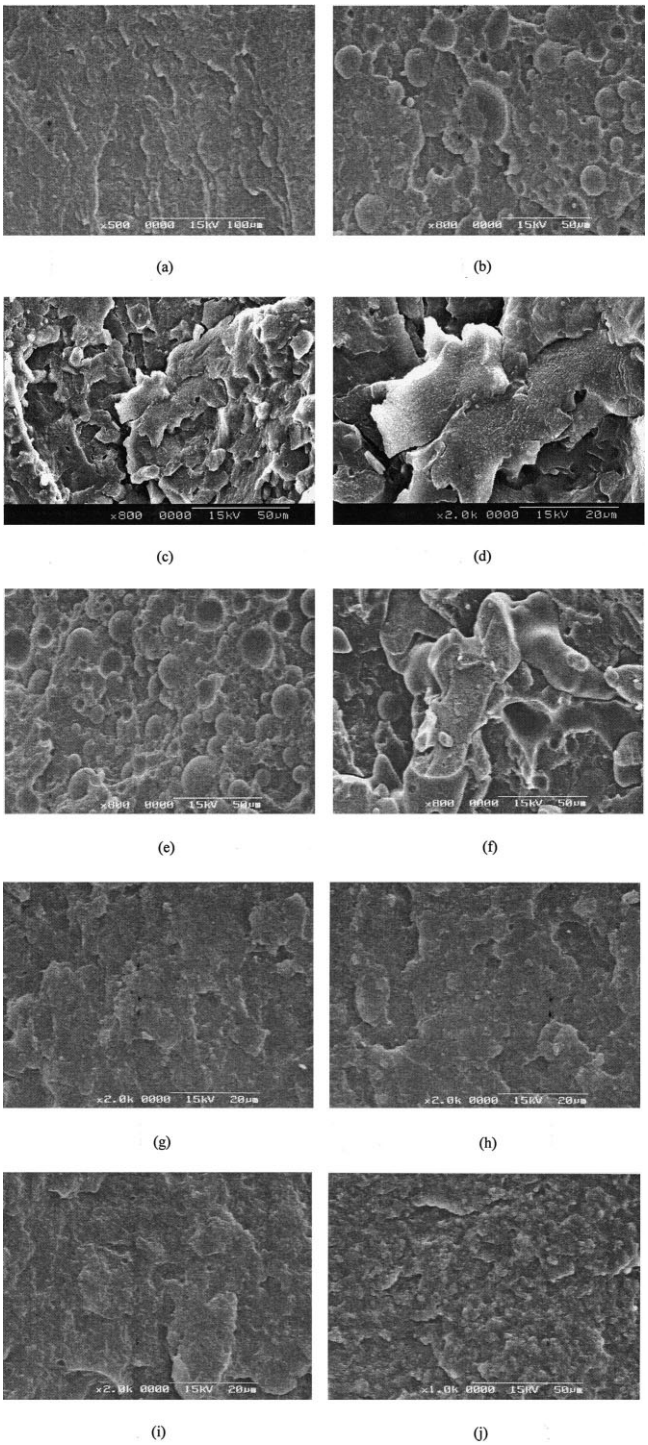

Figure 4 SEM micrographs of freeze-fractured surface of (a) PP, (b) PP/epoxy (70/30), (c) (d) PP/epoxy/CB (70/30/6.4) at different magnifications, (e) PP/epoxy/EMI-2,4 (70/30/1.2), (f) PP/epoxy/CB/EMI-2,4 (70/30/6.4/1.2), (g) PP/MAH-*g*-PP/epoxy (60/10/30), (h) PP/MAH-*g*-PP/epoxy/CB (60/10/30/6.4), (i) PP/MAH-*g*-PP/epoxy/EMI-2,4 (60/10/30/1.2), and (j) PP/MAH-*g*-PP/epoxy/CB/EMI-2,4 (60/10/30/6.4/1.2).

to it or the surface of that phase, the excess CB particles were forced to disperse in the other phase of the polymer blend with weaker affinity to it.[29–31] CB content of 6.4 phr has reached the percolation level in the epoxy phase, and the excess CB particles could disperse in the PP matrix. As mentioned above, CB particles can act as nucleating agents, accelerating the PP crystallization. Therefore, increasing CB content results in the increase in peak temperature and the overall rate of crystallization.

For the dynamically cured PP/epoxy (70/30) and PP/epoxy/CB (70/30/6.4) composites, Figures 4(e) and 4(f) show that the morphology is similar to that of the uncured composites. In PP/epoxy/EMI-2,4 (70/30/1.2), epoxy forms spherical particles in the PP matrix. The cured epoxy particles can act as nucleating agents, increasing the peak temperature and the overall rate of crystallization of the composite. Similarly, addition of CB results in the elongated structure of the epoxy phase where CB particles preferentially located. The elongated structure of epoxy greatly reduces its nucleation effect, leading to lower T_p.

Figures 4(g)–4(j) show the SEM micrographs of the PP/epoxy and PP/epoxy/CB composites containing the compatibilizer, MAH-*g*-PP. The addition of compatibilizer reduced the size of dispersed epoxy particles significantly. Fine epoxy particles with average diameter of about 1.0 μm are dispersed in the PP matrix, and the PP/epoxy interface is difficult to distinguish. The small particle size and illegible interface should be attributed to the improved compatibility between PP and the epoxy resin, resulting from the reaction of the maleic anhydride groups of MAH-*g*-PP with the hydroxyl or epoxy groups of the epoxy resin.[6] The epoxy particles with greatly reduced size can act as more effective nucleating agents than the larger ones, accelerating the crystallization of PP more effectively. As a result, the composites containing compatibilizer show significantly increased T_p values and relatively small $T_{onset} - T_p$ values. It is hard to judge the change in the epoxy particles' size after the addition of CB, from Figures 4(g)–4(j). The higher T_p in PP/MAH-*g*-PP/epoxy/CB (60/10/30/6.4) and its dynamically cured composite is probably due to the synergistic nucleation effect of the epoxy particles and the excess CB particles in the PP matrix on crystallization, since 6.4-phr CB has reached the percolation level in the epoxy phase. Arroyo et al.[2] have reported a similar synergistic effect of EPDM and aramid short fibers on the crystallization of PP.

As shown in Table II, all dynamically cured PP/epoxy and PP/epoxy/CB composites show lower T_p and greater $T_{onset} - T_p$ values than the corresponding uncured composites do, indicating that the nucleation effect of the epoxy particles in the dynamically cured composites is less prominent. It can be clearly seen in Figures 4(e), 4(i), and 4(j) that the dynamic cure results in smaller size of the epoxy particles, which could be explained as the dynamic cure of the epoxy resin avoided the aggregation of the epoxy particles in the

PP matrix.[6] The smaller epoxy particles in dynamically cured PP/epoxy and PP/epoxy/CB composites result in an increase in the number of the epoxy particles, leading to more coarsening morphology, as shown in the SEM micrographs. The decrease in the particle size of nucleating agents and the increase in the number of nucleating agents should facilitate the crystallization of PP. However, high content of nucleating agents created restrictions on the mobility of PP segments.[2,8] The decreased T_p values and the overall rate of crystallization in the dynamically cured composites imply that in the competition between the nucleation effect of epoxy particles and the restrictions on the mobility of PP segments caused by the greatly increased number of epoxy particles, the restriction effect plays the more important role.

Isothermal crystallization theories

The isothermal crystallization kinetics of polymers can be well approximated by the Avrami equation.[32,33]

$$X(t) = 1 - \exp[-K(T)t^n] \quad (1)$$

where $X(t)$ is the relative crystallinity at different crystallization times, the Avrami exponent n is a constant depending on the mechanism of nucleation and the form of crystal growth, and $K(T)$ is the crystallization kinetic constant related to nucleation and growth parameters. $X(t)$ can be calculated according to eq. (2).

$$X(t) = Q_t/Q_\infty = \int_0^t (dH/dt)dt \Big/ \int_0^\infty (dH/dt)dt \quad (2)$$

where Q_t and Q_∞ are the heat generated at time t and infinite time t_∞, respectively, and dH/dt is the rate of heat evolution.

The Avrami equation can be written as follows:

$$\log[-\ln(1 - X(t))] = n \log t + \log K(T) \quad (3)$$

From a graphic representation of $\log[-\ln(1 - X(t))]$ versus $\log t$, the Avrami exponent n (slope of the straight line) and the crystallization kinetic constant $K(T)$ (intersection with the y-axis) can be obtained. The half-time of PP crystallization ($t_{1/2}$) is defined as the time at which the relative crystallinity is 50%. It can be calculated according to the following equation.

$$t_{1/2} = [\ln 2/K(T)]^{1/n} \quad (4)$$

Usually, $t_{1/2}$ is used to characterize the rate of crystallization directly. The greater the value of $t_{1/2}$, the smaller the rate of crystallization is.

The crystallization thermodynamics and kinetics of polymer materials have been analyzed on the basis of the secondary nucleation theory of Hoffman and Lauritzen.[34,35]

$$(1/n)\log K(T) + \Delta F/2.3RT_c = A_0 - (4b_0\sigma\sigma_e T_m)/(2.3k_B \Delta H_f T_c \Delta T) \quad (5)$$

where $\Delta T = T^0{}_m - T_c$, σ and σ_e are the free energies per unit area of the surfaces of the lamellae parallel and perpendicular to the chain direction, respectively. ΔH_f is the enthalpy of fusion, b_0 is the distance between two adjacent fold planes, and k_B is the Boltzmann constant. The equilibrium melting temperature ($T^0{}_m$) can be obtained from the intersection of two straight lines. One is the plot of experimental melting temperature (T_m) versus T_c, and the second is a straight line with slope equal to one ($T_m = T_c$, Hoffman-Weeks plot).[36] If it is assumed that the spherulite nucleus density is independent of time, ΔT, blend composition, and T_m, A_0 can be taken as a constant. ΔF is the activation energy for the transport process at the liquid–solid interphase and can be calculated with a high precision from the Williams–Landel–Ferry (WLF) equation[37] given by the following expression:

$$\Delta F = \Delta F_{WLF} = (C_1 T_c)/(C_2 + T_c - T_g) \quad (6)$$

where C_1 and C_2 are constants whose values are assumed to be 17.24 kJ/mol and 51.6 K, respectively. T_g of pure PP was taken as 260 K.[1] When $(1/n)\log K(T) + \Delta F/2.3R\,T_c$ versus $T_m/T_c\,\Delta T$ is plotted, the value of $4b_0\,\sigma\,\sigma_e/k_B\,\Delta H_f$ can be calculated from the slope of the straight lines. b_0, σ, ΔH_f , and k_B have the following values given by the literature[1,8,38]: 5.24 Å, 11 mJ/m^2, 209 J/g, and 1.35×10^{-23} J/mol K, respectively. It is possible to calculate the value of the free energy of chain folding of PP lamellar crystals, σ_e, as a function of composite composition.

Isothermal crystallization of PP and the PP/CB composites

Figure 5 shows the plots of heat flow versus time during the isothermal crystallization of PP at different T_c's. It can be seen that the crystallization of PP is strongly affected by temperature. The time to reach the maximum degree of PP crystallization increases with increasing T_c, as already reported in the literature.[1,3–6,8]

Based on the change of heat flow with time, depicted in Figure 5, the development of the relative crystallinity of PP with time at different T_c's were recorded according to eq. (2), as shown in Figure 6(a). Accordingly, the plots of relative crystallinity versus time of the PP/CB composites with varied CB content

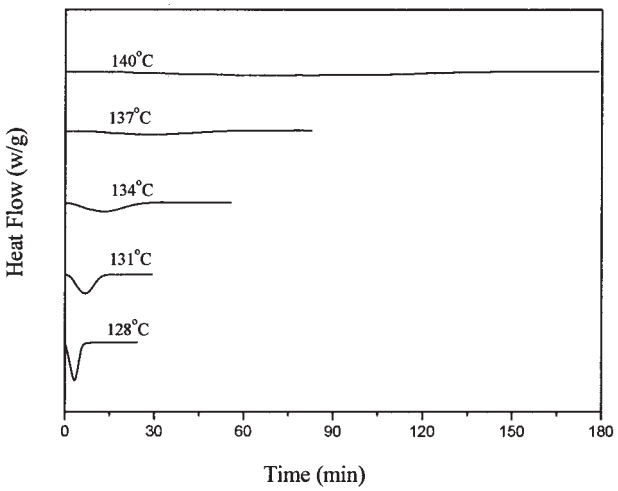

Figure 5 Heat flow versus time during isothermal crystallization of PP at different T_c's.

at different T_c's are recorded and shown in Figures 6(b) and 6(c). The half-time of PP crystallization ($t_{1/2}$) in pure PP and the PP/CB composites can be read conveniently from Figure 6. As can be seen, $t_{1/2}$ increases with increasing T_c. An increase of 12°C in T_c involves an increase of more than 10 times of $t_{1/2}$. Plots of log [−ln (1 − $X(t)$)] versus log t for PP and PP/CB composites are shown in Figure 7. The data exhibit good linearity in all cases. The values of the Avrami exponent n and the crystallization kinetic constant $K(T)$ of the samples were determined by the slope of the straight lines and the intersection with the y-axis. And the $t_{1/2}$ values were calculated according to eq. (4).

The values of $K(T)$, n, and $t_{1/2}$ of PP and the PP/CB composites determined from Figures 6 and 7 are listed in Table III. There is little difference between the experimental and the theoretical values of $t_{1/2}$. All PP/CB composites exhibit higher $K(T)$ and smaller $t_{1/2}$ than those of pure PP, indicating that the rate of

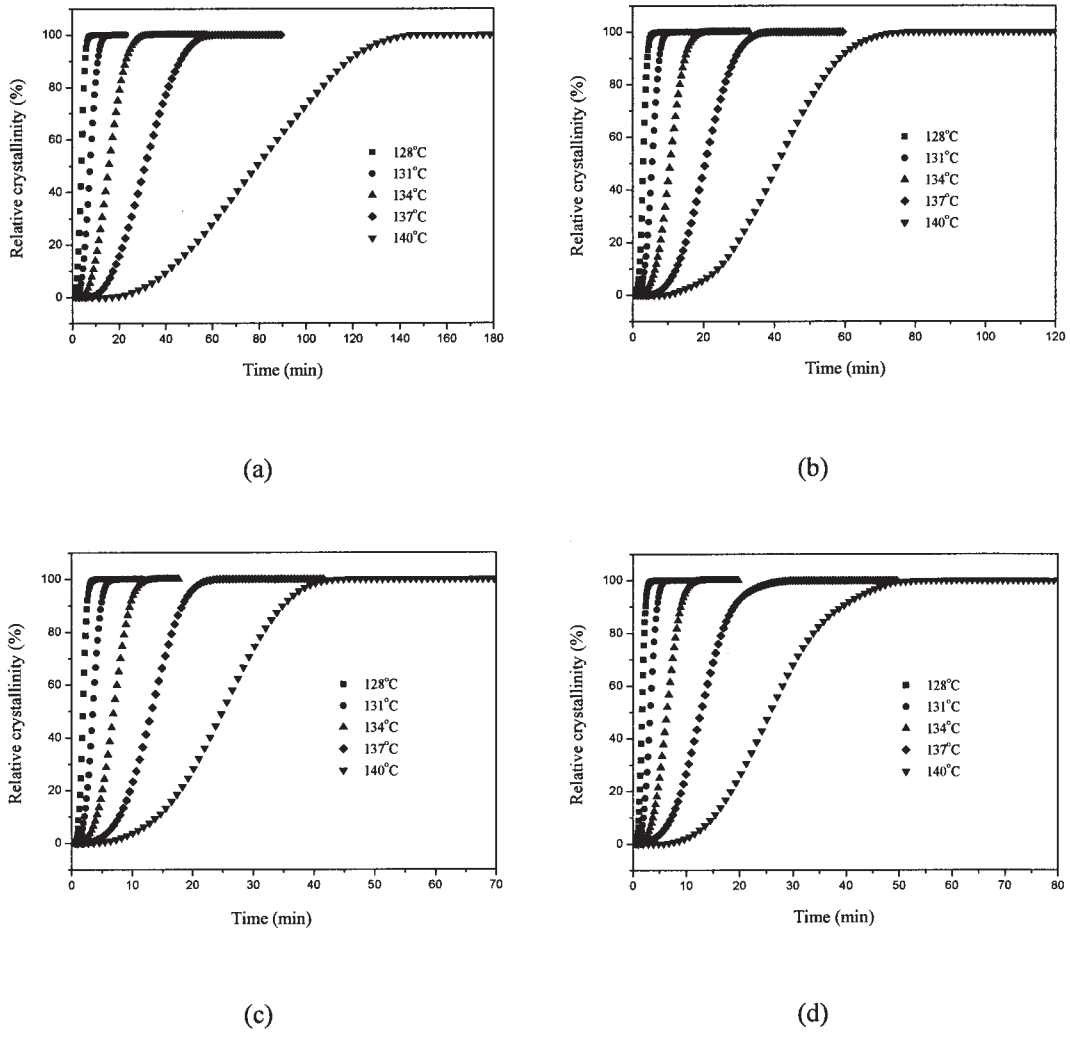

Figure 6 Development of the relative crystallinity with time during isothermal crystallization at different T_c's for (a) PP, (b) PP/CB (100/5.3), (c) PP/CB (100/10.0), and (d) PP/CB (100/17.7).

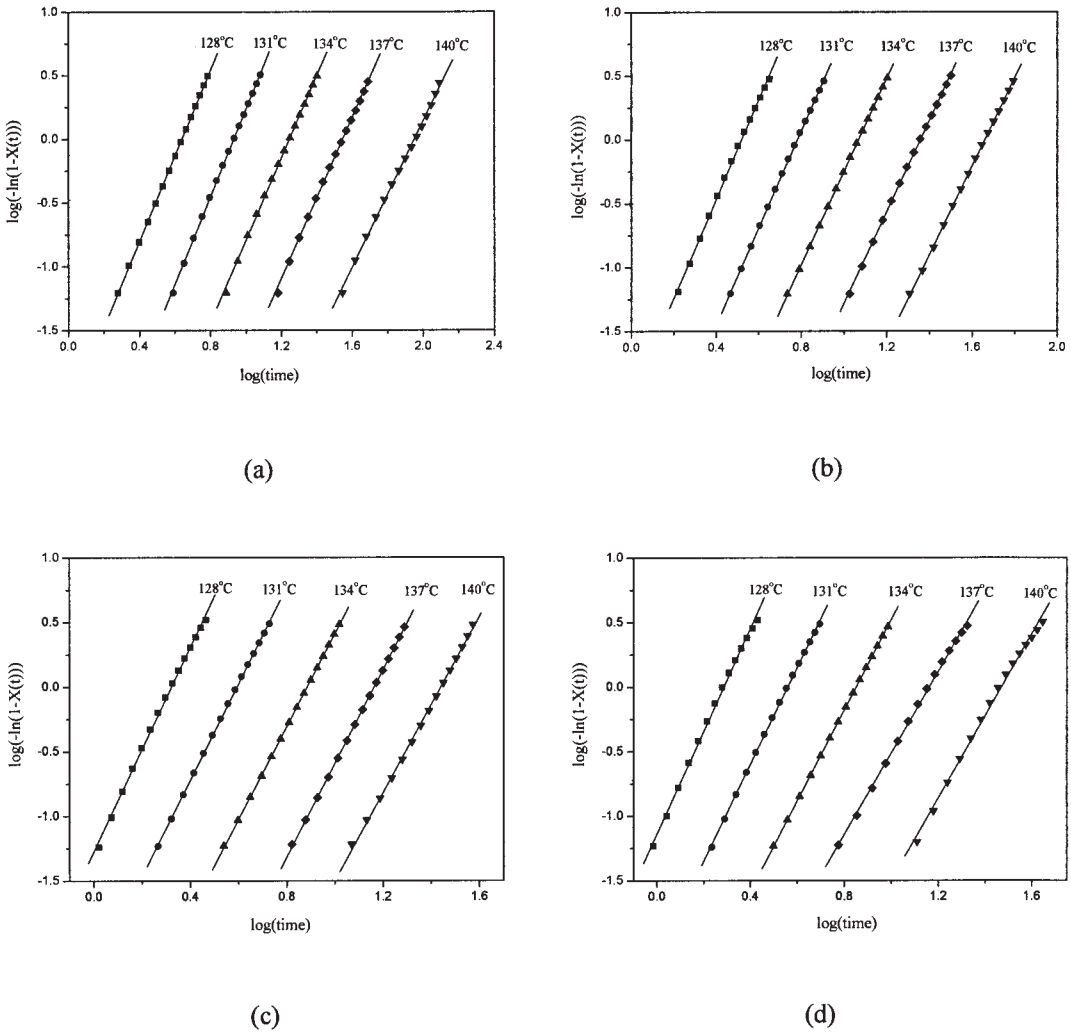

Figure 7 Avrami plots of PP and the PP/CB composites at different T_c's: (a) PP, (b) PP/CB (100/5.3), (c) PP/CB (100/10.0), and (d) PP/CB (100/17.7).

crystallization is faster in the PP/CB composites, which can be attributed to the nucleation effect of CB particles on the crystallization of PP. With increasing CB content at a given T_c, $K(T)$ increases and $t_{1/2}$ decreases. At a low CB content (5.3 phr), the change in $K(T)$ and $t_{1/2}$ is slight. When CB content reaches 10.0 phr, the increase in $K(T)$ and the decrease in $t_{1/2}$ are more perceivable. However, when CB content is increased from 10.0 to 17.7 phr, $K(T)$ is slightly increased but $t_{1/2}$ remains almost unchanged, confirming a compromise between the nucleation effect of CB and the restrictions caused by its own particles on the diffusion of crystallizing macromolecules.[25] It can also be deduced from Table III that $K(T)$ and $t_{1/2}$ are more affected by T_c than by the composition. In all cases, $K(T)$ decreases and $t_{1/2}$ increases with increasing T_c.

The Avrami exponent n depends on the nucleation process and the geometry of the growing crystals.[32,33] As shown in Table III, the values of n of the PP/CB composites are higher than that in pure PP. An increase in n is usually attributed to a change from instantaneous nucleation to sporadic nucleation in the literature.[1] n varies little with increasing CB content at a given T_c, and the value of about 3 indicates heterogeneous nucleation followed by a tridimensional spherutitic growth in a spherical form.[39]

After crystallization at different T_c, PP and the PP/CB composites were heated to 200°C at a rate of 10°C/min and the T_m values were recorded. The equilibrium melting temperatures (T^0_m) were calculated from the Hoffman–Weeks plots. The obtained T_m and T^0_m values of PP and the PP/CB composites are listed in Table III. In all cases, T_m increases with increasing T_c, which is directly related to the size of the PP crystals.[2] T^0_m of the PP/CB composites is lower than that of pure PP and decreases with increasing CB content. The plots of $(1/n) \log K(T) + \Delta F/2.3R\ T_c$ versus $T_m/T_c\ \Delta T$ of PP and the PP/CB composites are shown in Figure 8. The values of $4b_0\ \sigma\ \sigma_e/k_B\ \Delta H_f$ were calculated from the slope of the straight lines. The

TABLE III
Isothermal Crystallization Kinetics and Thermodynamics Parameters of PP and the PP/CB Composites

Composition	T_c (°C)	$K(T)$	n	$t_{1/2}$[a] (min)	$t_{1/2}$[b] (min)	T_m (K)	T_m^0 (K)	σ_e (mJ/m^2)
PP	128	7.08E-3	3.36	3.90	3.91	437.4	482.7	212
	131	6.31E-4	3.44	7.65	7.66	438.9		
	134	9.77E-5	3.22	15.65	15.70	440.5		
	137	1.31E-5	3.15	31.23	31.29	442.4		
	140	2.51E-6	2.87	78.72	78.68	444.0		
PP/CB (100/5.3)	128	9.77E-3	3.87	2.98	3.01	437.8	481.2	183
	131	1.07E-3	3.79	5.48	5.52	439.1		
	134	1.23E-4	3.66	10.56	10.59	440.8		
	137	1.32E-5	3.59	20.59	20.65	442.3		
	140	1.91E-6	3.45	40.83	40.88	444.2		
PP/CB (100/10.0)	128	0.054	3.95	1.90	1.91	437.6	478.8	173
	131	6.17E-3	3.73	3.53	3.55	439.1		
	134	6.76E-4	3.58	6.95	6.93	440.5		
	137	6.03E-5	3.62	13.20	13.23	442.2		
	140	1.23E-5	3.41	24.68	24.73	443.9		
PP/CB (100/17.7)	128	0.072	3.97	1.75	1.77	437.1	477.8	172
	131	7.94E-3	3.74	3.28	3.30	438.8		
	134	1.02E-3	3.51	6.40	6.41	440.3		
	137	2.14E-4	3.16	12.75	12.91	441.6		
	140	2.14E-5	3.18	24.13	24.20	443.6		

[a] Determined from Figure 6.
[b] Calculated from eq. (4).

values of the free energy of chain folding of PP lamellar crystals (σ_e) were calculated and the results are shown in Table III. It is clearly seen that σ_e of the PP/CB composites is lower than that of pure PP, and σ_e decreases with the increasing CB content. Similar to the $t_{1/2}$ values, σ_e remains almost unchanged when CB content is increased from 10.0 to 17.7 phr, which can be attributed to the above-mentioned compromise between the nucleation effect and the restrictions of CB particles on the crystallization of PP. The lower σ_e values in the PP/CB composites further confirm the nucleation effect of CB on the PP crystallization. According to Beck,[40] a good nucleating agent can reduce the value of σ_e.

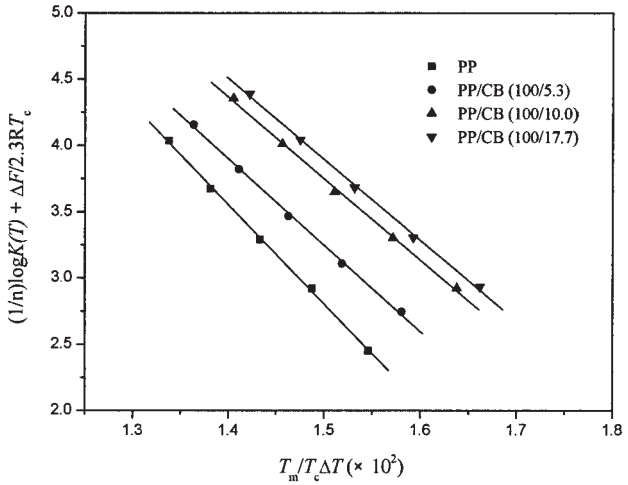

Figure 8 Plots of eq. (5) for PP and the PP/CB composites with varied CB content.

Isothermal crystallization of the PP/epoxy and PP/epoxy/CB composites

Figure 9 shows the development of the relative crystallinity with time during isothermal crystallization at different T_c's for the PP/epoxy and PP/epoxy/CB composites. The experimental values of $t_{1/2}$ can be directly read from the plots. Plots of log [−ln (1 − $X(t)$)] versus log t for the PP/epoxy and PP/epoxy/CB composites are shown in Figure 10. In all cases, the data exhibit good linearity. The values of the Avrami exponent n and the crystallization kinetic constant $K(T)$ of the samples were determined by the slope of the straight lines and the intersection with the y-axis. The theoretical values of $t_{1/2}$ were calculated according to eq. (4).

The values of $K(T)$, n, and $t_{1/2}$ of the PP/epoxy and PP/epoxy/CB composites are listed in Table IV. For a given composition, $K(T)$ decreases with increasing T_c. The experimental values of $t_{1/2}$ are in good accordance with the calculated values in all cases. PP/epoxy (70/30) shows higher $K(T)$ and smaller $t_{1/2}$ than pure PP at each T_c, which can be attributed to the nucleation effect of the epoxy particles dispersed in the PP matrix on the PP crystallization. After the incorporation of 6.4-phr CB into PP/epoxy (70/30), $K(T)$ decreases greatly. The $K(T)$ value of PP/epoxy/CB (70/30/6.4) is comparable with that of pure PP, or even smaller than that of PP at higher T_c. And the value of $t_{1/2}$ is

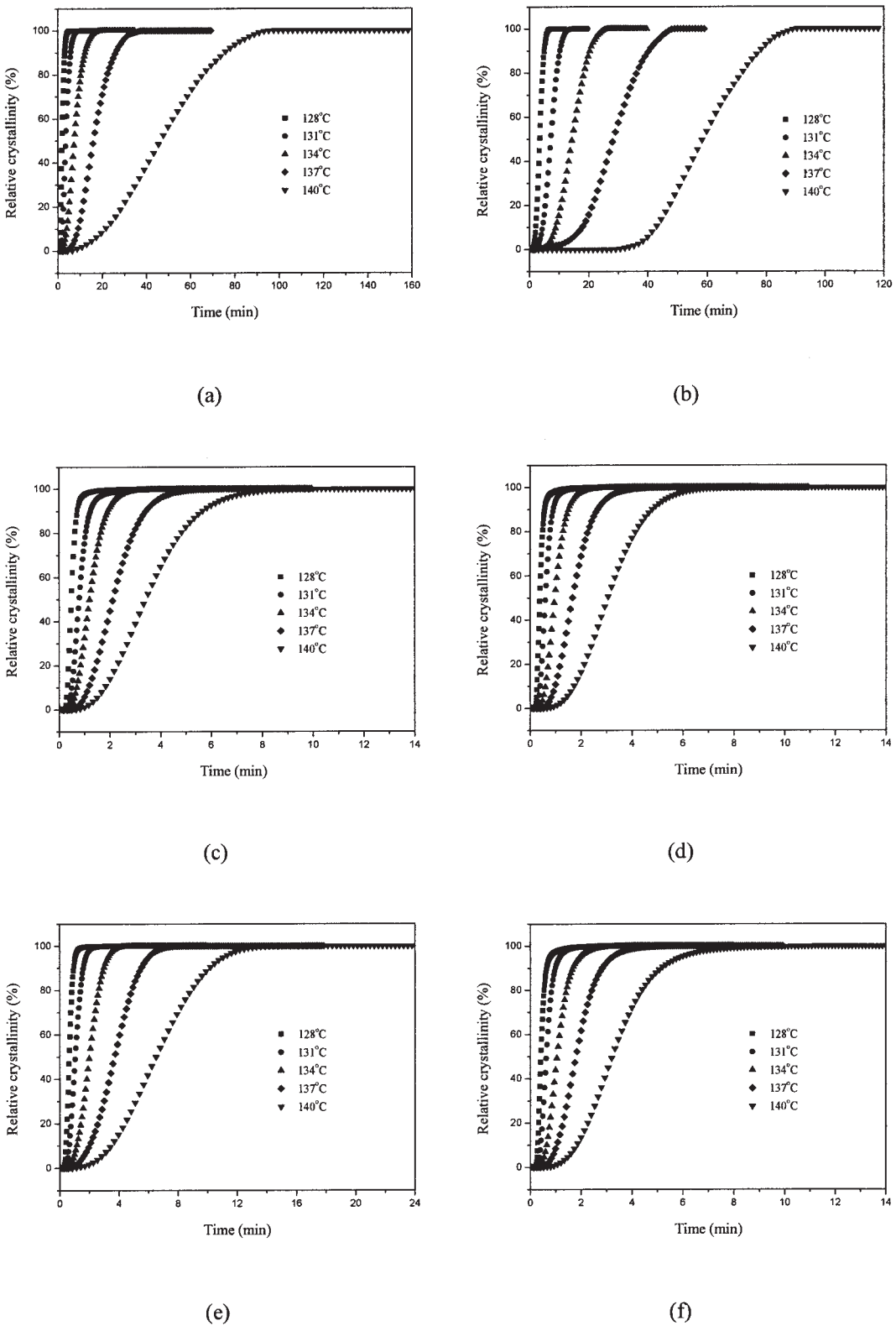

Figure 9 Development of the relative crystallinity with time during isothermal crystallization at different T_c's for (a) PP/epoxy (70/30), (b) PP/epoxy/CB (70/30/6.4), (c) PP/MAH-*g*-PP/epoxy (60/10/30), (d) PP/MAH-*g*-PP/epoxy/CB (60/10/30/6.4), (e) PP/MAH-*g*-PP/epoxy/EMI-2,4 (60/10/30/1.2), and (f) PP/MAH-*g*-PP/epoxy/CB/EMI-2,4 (60/10/30/6.4/1.2).

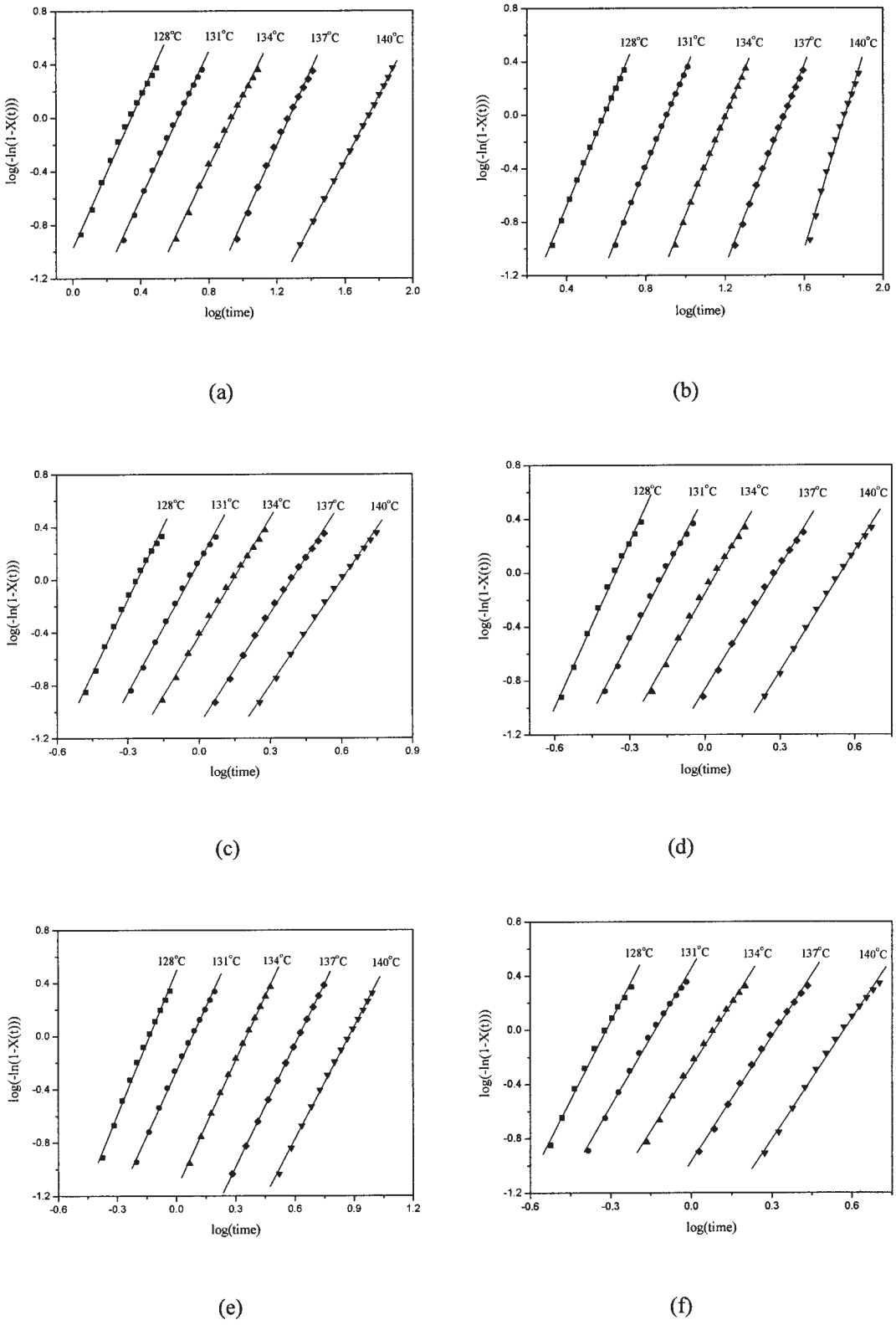

Figure 10 Avrami plots of the PP/epoxy and PP/epoxy/CB composites at different T_c's: (a) PP/epoxy (70/30), (b) PP/epoxy/CB (70/30/6.4), (c) PP/MAH-*g*-PP/epoxy (60/10/30), (d) PP/MAH-*g*-PP/epoxy/CB (60/10/30/6.4), (e) PP/MAH-*g*-PP/epoxy/EMI-2,4 (60/10/30/1.2), and (f) PP/MAH-*g*-PP/epoxy/CB/EMI-2,4 (60/10/30/6.4/1.2).

TABLE IV
Isothermal Crystallization Kinetics and Thermodynamic Parameters of the PP/Epoxy and PP/Epoxy/CB Composites

Composition	T_c (°C)	$K(T)$	n	$t_{1/2}$[a] (min)	$t_{1/2}$[b] (min)	T_m (K)	T_m^0 (K)	σ_e (mJ/m^2)
PP/epoxy (70/30)	128	0.10	2.83	1.88	1.98	437.2	478.1	196
	131	0.020	2.75	3.56	3.63	438.8		
	134	3.31E-3	2.64	7.36	7.57	440.4		
	137	2.57E-4	2.82	16.33	16.47	441.8		
	140	6.46E-5	2.42	46.15	46.30	443.7		
PP/epoxy/CB (70/30/6.4)	128	7.94E-3	3.55	3.48	3.52	437.2	486.7	220
	131	5.25E-4	3.62	7.23	7.28	438.8		
	134	4.07E-5	3.64	14.38	14.54	440.5		
	137	2.40E-6	3.75	28.30	28.59	442.3		
	140	1.86E-9	4.33	58.65	59.51	444.4		
PP/MAH-*g*-PP/epoxy (60/10/30)	128	9.12	3.71	0.49	0.50	437.1	453.7	57
	131	1.35	3.30	0.80	0.82	438.0		
	134	0.37	2.98	1.20	1.23	438.8		
	137	0.079	2.81	2.12	2.16	439.9		
	140	0.026	2.64	3.42	3.45	440.9		
PP/MAH-*g*-PP/epoxy/CB (60/10/30/6.4)	128	28.84	3.99	0.39	0.40	437.1	450.1	50
	131	3.72	3.57	0.60	0.62	437.9		
	134	0.71	3.25	0.97	0.99	438.8		
	137	0.14	3.03	1.67	1.70	439.4		
	140	0.024	2.98	3.05	3.09	440.2		
PP/MAH-*g*-PP/epoxy/EMI-2,4 (60/10/30/1.2)	128	3.09	3.61	0.65	0.66	437.2	455.4	70
	131	0.54	3.24	1.07	1.08	438.0		
	134	0.071	3.22	2.02	2.03	439.2		
	137	0.013	3.07	3.67	3.69	440.1		
	140	0.0034	2.83	6.52	6.55	441.2		
PP/MAH-*g*-PP/epoxy/CB/EMI-2,4 (60/10/30/6.4/1.2)	128	16.60	3.86	0.43	0.44	437.0	452.5	52
	131	2.88	3.40	0.64	0.66	437.9		
	134	0.54	3.13	1.06	1.08	438.7		
	137	0.11	3.06	1.80	1.82	439.6		
	140	0.020	2.96	3.23	3.29	440.5		

[a] Determined from Figure 9.
[b] Calculated from eq. (4).

greater than that of PP/epoxy (70/30). This is probably due to the formation of elongated structure of the dispersed epoxy phase shown in Figures 4(c) and 4(d), which greatly reduced the nucleation effect of the epoxy resin. The PP/epoxy and PP/epoxy/CB composites containing compatibilizer (MAH-*g*-PP) show significant increase in the $K(T)$ values, which is about a thousand times greater than that of pure PP at different T_c's. The $t_{1/2}$ values are significantly decreased after the addition of MAH-*g*-PP. This can be explained by the significantly reduced size of epoxy particles resulted from the well-improved compatibility between PP and the epoxy resin. The much smaller epoxy particles in the PP matrix can act as more effective nucleating agents, increasing $K(T)$ and decreasing $t_{1/2}$ significantly. For the compatibilized composites, the addition of CB further increases $K(T)$ and decreases $t_{1/2}$, indicating CB has a synergistic effect on accelerating the crystallization of PP. The dynamically cured PP/MAH-*g*-PP/epoxy and PP/MAH-*g*-PP/epoxy/CB composites exhibit lower $K(T)$ and greater $t_{1/2}$ values than the corresponding uncured composites do, which could be attributed to the restriction on the mobility of PP caused by the significant increase in the number of epoxy particles after dynamic cure. As seen in Table IV, the maximum $K(T)$ and the minimum $t_{1/2}$ are obtained in the PP/MAH-*g*-PP/epoxy/CB (60/10/30/6.4) composite. It can also be deduced from Table IV that $K(T)$ and $t_{1/2}$ are more affected by T_c than by the composition for the composites containing MAH-*g*-PP. $K(T)$ decreases and $t_{1/2}$ increases with increasing T_c at a given composition.

The Avrami exponent n of the PP/epoxy and PP/epoxy/CB composites varies with the composition. However, n varies a little in the composites containing compatibilizer at different T_c's. The value of about 3

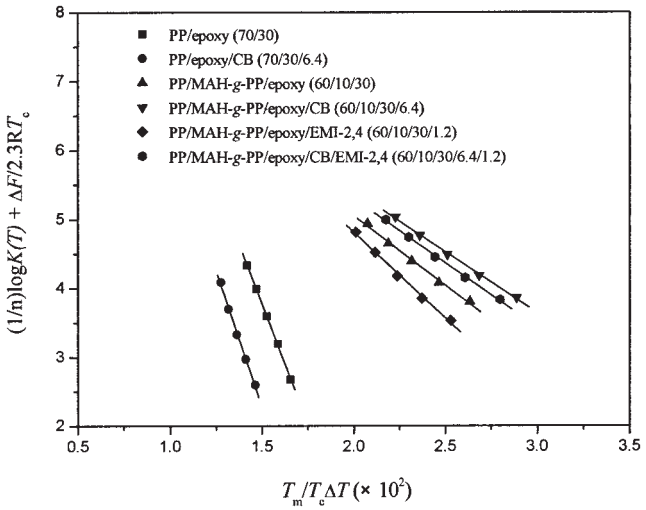

Figure 11 Plots of eq. (5) for the PP/epoxy and PP/epoxy/CB composites.

that indicates heterogeneous nucleation followed by a tridimensional spherutitic growth in a spherical form[39] takes place during the isothermal crystallization.

The plots of $(1/n)\log K(T) + \Delta F/2.3RT_c$ versus $T_m/T_c\Delta T$ of the PP/epoxy and PP/epoxy/CB composites are shown in Figure 11. The values of T_m, T^0_m, and σ_e are listed in Table IV. In all cases, T_m increases with increasing T_c. σ_e of PP/epoxy (70/30) is lower than that of pure PP, 212 mJ/m^2 (Table III). Addition of CB increases the value of σ_e to 220 mJ/m^2, which is higher than that of pure PP. For the PP/epoxy and PP/epoxy/CB composites containing compatibilizer MAH-*g*-PP, σ_e decreases significantly, confirming that the epoxy particles of smaller size act as much more effective nucleating agents than the greater epoxy particles. The σ_e values of the compatibilized composites are similar to that previously reported.[6] Addition of CB lowers σ_e, and dynamic cure increases σ_e, which can be attributed to the synergistic effect of CB on the PP crystallization and the restriction of increased number of epoxy particles on the mobility of PP segments after dynamic cure, respectively. PP/MAH-*g*-PP/epoxy/CB (60/10/30/6.4) has the minimum σ_e value.

CONCLUSIONS

CB can act as nucleating agents, increasing the peak temperature and the overall crystallization rate of the PP/CB composites. The isothermal crystallization studies show the PP/CB composites exhibit higher $K(T)$, smaller $t_{1/2}$, and lower σ_e than that of pure PP. Increasing CB content accelerates the crystallization of PP. However, high CB content tends to cause restriction on the PP crystallization. The values of n (~3) indicate heterogeneous nucleation followed by a tridimensional spherutitic growth in a spherical form. In PP/epoxy (70/30), the dispersed epoxy particles can act as nucleating agents, accelerating the crystallization of the composite. Addition of CB into PP/epoxy (70/30) results in the preferential distribution of CB in the epoxy phase, changing the spherical epoxy particles into elongated structure, and thus decreases the nucleation effect of epoxy particles. Addition of compatibilizer MAH-*g*-PP reduces the size of epoxy particles significantly. The smaller epoxy particles act as more effective nucleating agents, increasing the peak temperature and the overall rate of the crystallization noticeably. In the compatibilized PP/epoxy/CB composites, CB has a synergistic effect with epoxy particles on the crystallization of PP. In the dynamically cured PP/epoxy and PP/epoxy/CB composites, the further decreased size of epoxy particles increases the number of the epoxy particles greatly, which could cause restrictions on the mobility of PP segments and slow down the PP crystallization. The studies on isothermal crystallization kinetics show that all PP/epoxy and PP/epoxy/CB composites exhibit higher $K(T)$ and smaller $t_{1/2}$ than that of pure PP. The values of the Avrami exponent n are about 3, indicating tridimensional spherutitic growth. The composites containing MAH-*g*-PP show remarkably increased $K(T)$ and rate of crystallization. The σ_e value of the compatibilized composites is much lower than that of pure PP. The PP/MAH-*g*-PP/epoxy/CB (60/10/30/6.4) composite shows the maximum $K(T)$ and the minimum $t_{1/2}$ and σ_e values.

References

1. Avalos, F.; Lopez-Manchado, M. A.; Arroyo, M. Polymer 1996, 37, 5681.
2. Arroyo, M.; Zitzumbo, R.; Avalos, F. Polymer 2000, 41, 6351.
3. Lopez-Manchado, M. A.; Torre, L.; Kenny, J. M. J Appl Polym Sci 2001, 81, 1063.
4. Lopez-Manchado, M. A.; Biagiotti, J.; Torre, L.; Kenny, J. M. J Therm Anal Calorim 2000, 61, 437.
5. Li, C. Q.; Tian, G. H.; Zhang, Y.; Zhang, Y. X. Polym Test 2002, 21, 919.
6. Jiang, X. L.; Zhang, Y.; Zhang, Y. X. J Polym Sci Part B: Polym Phys 2004, 42, 1181.
7. Saroop, M.; Mathur, G. N. J Appl Polym Sci 1999, 71, 151.
8. Arroyo, M.; Lopez-Manchado, M. A.; Avalos, F. Polymer 1997, 38, 5587.
9. Bogoeva-Gaceva, G.; Janevski, A.; Mader, E. Polymer 2001, 42, 4409.
10. Wang, C.; Liu, C. R. Polymer 1999, 40, 289.
11. López-Manchado, M. A.; Arroyo, M. Polymer 2000, 41, 7761.
12. Albano, C.; Papa, J.; Ichazo, M.; González, J.; Ustariz, C. Compos Struct 2003, 62, 291.
13. Medeiros, E. S.; Tocchetto, R. S.; Carvalho, L. H.; Santos, I. M. G.; Souza, A. G. J Therm Anal Calorim 2001, 66, 523.
14. Qian, J. S.; He, P. S.; Nie, K. M. J Appl Polym Sci 2004, 91, 1013.
15. Lin, Z. D.; Qiu, Y. X.; Mai, K. C. J Appl Polym Sci 2004, 92, 3610.
16. Bhattacharyya, A. R.; Sreekumar, T. V.; Liu, T.; Kumar, S.; Ericson, L. M.; Hauge, R. H.; Smalley, R. E. Polymer 2003, 44, 2373.

17. Maiti, P.; Nam, P. H.; Okamoto, M.; Hasegawa, N.; Usuki, A. Macromolecules 2002, 35, 2042.
18. Mubarak, Y.; Harkin-Jones, E. M. A.; Martin, P. J.; Ahmad, M. Polymer 2001, 42, 3171.
19. Narkis, M.; Ram, A.; Flashner, F. J Appl Polym Sci 1978, 22, 1163.
20. Miyasaka, K.; Watanabe, K.; Jojima, E.; Aida, H.; Sumita, M.; Ishikawa, K. J Mater Sci 1982, 77, 1610.
21. Zois, H.; Apekis, L.; Omastová, M. Macromol Symp 2001, 170, 249.
22. Cheah, K.; Forsyth, M.; Simon, G. P. J Polym Sci Part B: Polym Phys 2000, 38, 3106.
23. Tchoudakov, R.; Breuer, O.; Narkis, M. Polym Eng Sci 1996, 36, 1336.
24. Segal, E.; Tchoudakov, R.; Narkis, M.; Siegmann, A. J Polym Sci Part B: Polym Phys 2003, 41, 1428.
25. Mucha, M.; Marszalek, J.; Fidrych, A. Polymer 2000, 41, 4137.
26. Acosta, J. L.; González, L.; Del Río, C.; Ojeda, C.; Rodríguez, A. J Appl Polym Sci 2001, 79, 2136.
27. Acosta, J. L.; González, L.; Del Río, C.; Ojeda, C.; Rodríguez, A. J Appl Polym Sci 2002, 84, 646.
28. Gupta, A. K.; Purwar, S. N. J Appl Polym Sci 1984, 29, 1595.
29. Zhang, M. Q.; Yu, G.; Zeng, H. M.; Zhang, H. B.; Hou, Y. H. Macromolecules 1998, 31, 6724.
30. Mironi-Harpaz, I.; Narkis, M. J Appl Polym Sci 2001, 81, 104.
31. Feng, J. Y.; Chan, C. M. Polymer 2000, 41, 4559.
32. Avrami, M. J Chem Phys 1939, 7, 1103.
33. Avrami, M. J Chem Phys 1941, 9, 177.
34. Hoffman, J. D. Soc Plast Eng Trans 1964, 4, 315.
35. Hoffman, J. D.; Miller, R. L. Polymer 1997, 38, 3151.
36. Hoffman, J. D.; Weeks, J. J. J Chem Phys 1962, 37, 1723.
37. Williams, M. L.; Landel, R. F.; Ferry, J. D. J Am Chem Soc 1965, 77, 3701.
38. Avalos, F.; Lopez-Manchado, M. A.; Arroyo, M. Polymer 1998, 39, 6173.
39. Mandelkern, L. Crystallization of Polymers; McGraw-Hill: New York, 1964.
40. Beck, H. N. J Appl Polym Sci 1975, 19, 371.